Supplementary Material (ESI) for Chemical Communications

SUPPLEMENTARY INFORMATION

Nanomechanical properties of reversed surfactant bilayers formed in micrometre-sized holes

Jian Jin, Yukihiro Sugiyama, Keita Mitsui, Hideo Arakawa, and Izumi Ichinose*

1. Experimental details on characterization of DFFs

Preparation procedures of DFFs have been described in detail in *Angew. Chem. Int. Ed.* **2005**, *44*, 4532–4535. If not specified, the films were prepared on QUANTIFOIL® microgrids (Q250-CR2). We examined more than 500 holes by SEM to determine the film coverage, which is listed in Table 1 of our article.

Thicknesses of DPC and C18NSi films were determined by TEM. First, a 2-nm thick Pt layer was deposited on one side of the films by ion sputtering. The microgrid was cut in half and set on a TEM sample holder. The film along the cutting line was readily warped by irradiation of electron beam, since it was detached from the side walls of the hole. Then, the surfactant bilayer was clearly observed at the edge of the bending part. The thickness of C18NSi film was estimated to be 4.7±0.6 nm (Figure S1). This value is a little smaller than double of the molecular length of C18NSi (2.7 nm). Probably, the alkyl chains are slightly tilted in the reversed bilayer structure. Thicknesses of DTAB and DMIC films were estimated from their cross-sectional SEM observations.

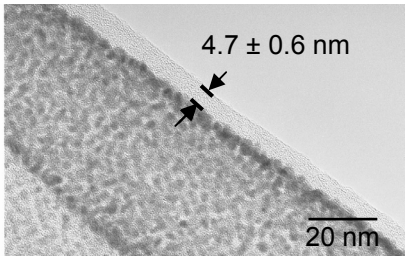

Figure S1 Side-view TEM image of the bending part of C18NSi film.

2. Force–indentation analysis

Figure S2 explains the difference of deflection–displacement curves of stiff and soft samples, where samples approach to AFM tip in a direction from right to left of the X axis. On a stiff sample, the deflection of cantilever is proportional to the sample displacement during the tip contacts the sample surface. On the other hand, a soft sample is deformed by the tip with increasing loading force. Therefore, the deflection of the cantilever on a soft sample is smaller than that on a stiff sample and the difference between them is corresponding to the indentation of the soft sample. This provides the base for analyzing the mechanical properties of soft materials.

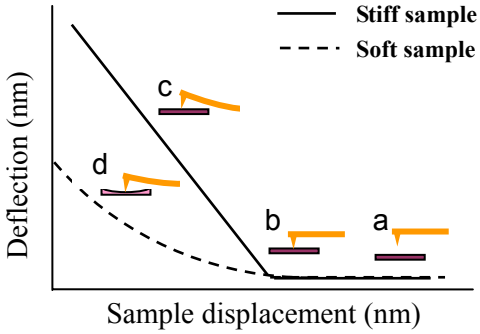

Figure S2 Schematic deflection–displacement curves of stiff and soft samples and pictures of cantilever on the samples. (a) The sample comes close to an AFM tip. (b) The surface touches the tip. (c) Stiff sample loads force on the tip without indentation. (d) Soft sample deforms with increasing loading force.

For the measurement of force–indentation (F–δ) curves, a pyramidal AFM tip, Olympus silicon nitride micro-cantilever (catalog number: OMCL-RC800PSA-1), was used. Young's modulus was obtained by fitting the curves with Hertzian model. To verify the adequacy of the curve fitting, we also examined the relationship of F and $\delta^{3/2}$. The Hertzian model gives a linear relationship between F and $\delta^{3/2}$ as follows:

$$F = E'\delta^{\frac{3}{2}} \qquad E' = \frac{4}{3}\frac{E}{(1-\nu^2)}\sqrt{R}$$

, where R and ν are fixed parameters. The elastic modulus (E) is obtainable from the slope of F–$\delta^{3/2}$ curve. Figure S3 shows a typical F–$\delta^{3/2}$ curve of a DPC film. The fitting curve starts from the zero points for X ($\delta^{3/2}$) and Y (F) axes. The experimental data showed a linear increase in the indentation range of 1.5–8.5 in a scale of 10^{-13} ($m^{3/2}$), which is corresponding to the indentation range of 3–9 nm. This indicates that the curve fitting of Figure 3A in our article is adequate.

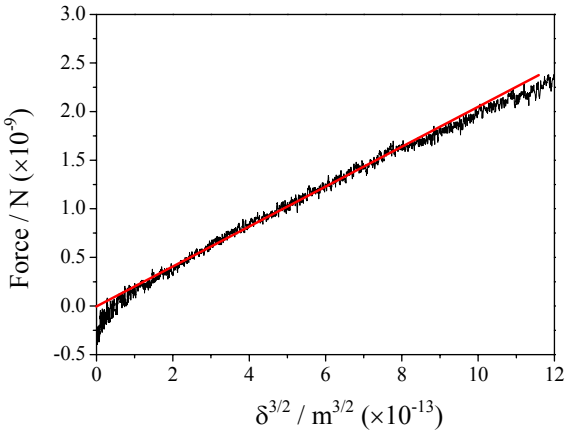

Figure S3 F-$\delta^{3/2}$ curve of DPC film (black line) and the fitting curve (red line).

3. Positioning method of AFM tip

As described in our article, DFFs were readily damaged in a contact mode AFM imaging. Therefore, we could not scan the films before measuring the force curves. In order to measure the force curves just on the films, two processes were required (Figure S4). First, up and down parts of a certain area were scanned in a contact mode to obtain the images of holes (A). These images were used for locating an AFM tip just on the film (B), and then the force curves were measured in a contact mode.

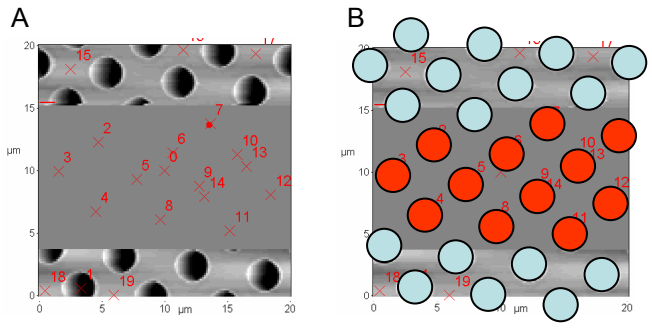

Figure S4 Two processes for the measurements of force curve.

4. Thermal stability of various DFFs

The thermal stability of DFFs was statistically analyzed by monitoring the changes of film coverage (Figure S5). The films were prepared on a copper microgrid with a perforated polymer membrane and heated for 20 min at a given temperature. Then the percentage of the films remained after heating was examined by SEM for more than 500 holes. As shown in Figure S5, DPC, DTAB, and C18NSi showed thermal stability higher than 150 °C. That of DMIC was 90 °C. The coverage tends to sharply decrease at certain critical temperature, indicating high molecular cooperativity in the reversed bilayer structure.

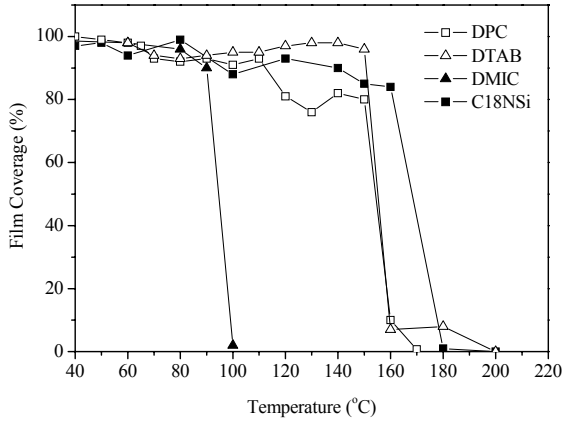

Figure S5 Temperature dependence of the coverage of DPC, DTAB, DMIC, and C18NSi films.